Engineered Science
DOI: https://dx.doi.org/10.30919/es979

A Novel Hybrid Metaheuristic Approach to Parameter Estimation of Photovoltaic Solar Cells and Modules

Thira Jearsiripongkul,[1,*] Pradya Prempraneerach,[1] Mahdiyeh Eslami[2,*] and Mohammad Amin Moarrefi[3]

Abstract

In order to determine the unknown parameters of the photovoltaic (PV) model, this paper introduces a novel evolutionary hybrid optimization technique that combines the single candidate optimizer (SCO) and the chaotic sand cat optimizer (CSCO). The addition of a chaotic structure to the SCO approach improves its capacity to explore while hindering earlier convergence. The effective global search capability of the CSCO and the effective local search capability of the SCO technique is credited with the effectiveness of the suggested hybrid strategy, known as the CSCSC. The effectiveness of the CSCSC algorithm is assessed using mathematical test functions, and the outcomes are contrasted with those of the conventional SCO and a number of efficient optimization methods. Following that, the CSCSC method is used to obtain the PV parameters. It is said that finding these parameters is an objective function whose differences between estimated and experimental data should be kept to a minimum. To assess how well the CSCSC obtains parameters, the single diode, double diode, and PV module models are employed. Based on the results of the numerical testing, it can be concluded that the newly presented algorithm performs better than previously described approaches in the academic literature when it comes to producing optimal solutions. The simulation findings demonstrate that the novel optimization procedure, which has the lowest root mean square error, offers better optimal solutions than earlier techniques for all varieties of solar cells.

Keywords: Solar cells; Single candidate optimizer; Sand cat optimization; PV modules; Hybrid.
Received: 15 September 2023; Revised: 29 September 2023; Accepted: 03 October 2023.
Article type: Research article.

1. Introduction

Due to its abundance of resources, safety, lack of pollution, dependability, and several other benefits, solar energy has grown in importance as a key renewable clean energy research and development project in response to serious environmental pollution and the worldwide energy deficit.[1] Renewable-energy system electrical grids need to be more flexible and dynamic than conventional grids to increase their contribution to total energy generation and overcome the challenges of intermittency and varying availability at specific locations.[2-5] Many countries will need to produce power using renewable energy sources due to the effects of global warming getting worse and the depletion of fossil fuels.[6,7] One choice is solar photovoltaic (PV) systems, which are composed mostly of solar cells. Due to its abundance and lack of pollutant production, solar energy is among the most promising renewable energy sources.[8] To maximize energy conversion, an ideal based on experimental current and voltage data is needed for evaluating and predicting PV characteristics.[9] In PV application research, performance and reliability must be assessed. The key element determining the actual performance characteristics of the separate components is the electrical performance of PV cell.[10] Still, the proficiency of a PV generation system is extremely subject to environmental conditions such as partial shade, climate, temperature, irradiation, and other external factors, as well as unstable output power.[11] It is critical to examine a set of PV module (PVM) characteristics in order to replicate real current and voltage. The static PV models presently used to describe PV contain the single diode model (SDM), double diode model

[1] *Department of Mechanical Engineering, Thammasat School of Engineering, Faculty of Engineering, Thammasat University, Pathumthani 12121, Thailand.*
[2] *Department of Electrical Engineering, Kerman Branch, Islamic Azad University, Kerman 7635131167, Iran.*
[3] *Department of mathematics, Kerman Branch, Islamic Azad university, Kerman 7635131167, Iran.*
**Email:* jthira@engr.tu.ac.th (T. Jearsiripongkul); m.eslami@iauk.ac.ir (M. Eslami)

(DDM), and PVM model.[12] It requires mathematical formulas and parameter selection to simulate solar PV systems. Unfortunately, no one knows the values of these parameters, which limits the applicability of all of these models.[13] The diode amount, ideality factor, series resistances, shunt resistance, and other elements comprise the performance parameter. The I-V data points are often added to the model equations to create the nonlinear equations, which are then solved to get the unknown parameters.[14] The restrained least squares approach, the best quick descent method, Newton's method, and Newton's suggested method are some examples of numerical analytic techniques that are frequently used to solve nonlinear problems.[15,16] The aforementioned approaches, however, rely on gradient information to tackle the issue and have a number of drawbacks, including susceptibility to noise, poor accuracy, method complexity, and so on. Additionally, some knowledge of numerical analysis is necessary for the operator to choose the iteration stages, *etc*.

In recent years, the scientific topic of optimization has gained significant prominence as a cost-effective methodology for identifying optimal solutions to complex problems. The categorization of optimization approaches into four groups has been based on the type of inspiration. As a result, metaheuristic algorithms (MAs) have been developed to address the parameter estimation optimization problem for solar PV models in relation to numerical analytic approaches.[17-29] The existing body of literature demonstrates the successful implementation of several MA methods for the extraction of PV parameters.[30-37] These methods include the Genetic Algorithm (GA),[38] Particle Swarm Optimization (PSO),[39] Improved JAYA (IJAYA),[40] Multi-Verse Optimization (MVO),[28] Tunicate Swarm Algorithm (TSA),[41] Grey Wolf Optimizer (GWO),[30] Resistance–Capacitance Optimization Algorithm (RCOA),[31] Gradient-Based Optimizer (GBO),[32] Gaussian and Cauchy Mutation-based HGSO (GCMHGSO)[42] and Salp Swarm Algorithm (SSA).[35,43]

In contrast to their conventional counterparts, these techniques have demonstrated superior accuracy and less sensitivity to the initial prediction. Several techniques and their respective modifications are commonly employed for the direct estimation of parameters in different PV models. It is important to note that the Root-Mean-Square-Error (RMSE) of the current was employed as the fitness function for minimization in all of the strategies. Enhancement of conjunction, protection from initial guess, lack of singularity condition, and evaluation of all I-V data points rather than important spots on the I-V curve are a few benefits of MA techniques. The rate of convergence, precision, and implementation complexity are all important factors to take into account while choosing these optimization techniques. Though, numerous better MAs have been widely proposed by researchers, and the MAs can readily enter the local optimum. Accordingly, several studies have been conducted to enhance the effectiveness and performance of the original MA and tailor them to a particular application.[44-47] The literature study shows that it is very desirable to provide fresh MAs to address real-world problems. In spite of these advancements, challenges continue within this rapidly evolving sector. One of the foremost challenges being faced pertains to the requirement of substantial volumes of superior-quality data for training models, alongside issues concerning convergence, local optima, and overfitting within MAs methodologies. Nevertheless, the persistent study and innovation in the field continue to drive the search for solutions to these issues, hence fostering further advancements in the estimate of parameters for solar PV cells and modules. It is important to emphasize that the discovery of universal solutions cannot be guaranteed, as every heuristic-based framework relies on random initialization for commencing and updating each method. Hence, it is evident that none of the existing strategies can provide a definitive assurance of attaining a comprehensive worldwide solution. Nevertheless, there remains room for further advancement in this domain as scholars strive to build novel algorithms that enhance the probability of avoiding entrapment in local minima. The limited search capability of the fundamental algorithm results in its tendency to converge prematurely by collapsing into local optima rapidly. The equation pertaining to individual mutations encounters challenges in effectively reconciling the competing objectives of exploitation and investigation. In complex scenarios with limited iterations, the fundamental iterations encounter challenges in achieving global optima.

A recently industrialized bioinspired MA technique called the sand cat optimizer (SCO) approach is encouraged by the sand cat's (SC) search and hunting activity.[48] The invention of the SCO was motivated by the low-frequency noise-detecting actions of SCs to locate prey.[48] In terms of obtaining the best outcomes, SCO surpasses other strategies and is ideally suited to real-world optimization settings. The updated version of the original SCO that is described in this study, the chaotic SCO (CSCO), contains chaotic sequences to increase the algorithm's capability for searching and exploring. Any MA must be processed with stability between exploitation and exploration during the search strategy in order to function at its best. As a global search strategy, CSCO examines a large area; as a result, when used exclusively, it could not produce the best results. However, when the objective function is

complicated and has a lot of variables, CSCO frequently experiences the same problem as other MAs: being stuck in local minima. This study has utilized a novel hybrid approach in order to attain optimal and accurate parameter estimates for PV cells and modules. A hybrid method based on CSCS and Single Candidate Optimizer (SCO) has been created to address this flaw.

SCO, a search engine strategy, uses the local but may do a thorough search.[49] Due to the different capacities of various approaches, there is room for hybridization. As a result of the above, a combination of CSCO and SCO approaches known as CSCSC was developed and is currently being utilized in the present effort to identify the least amount of RMSE necessary to extract the PV parameters. The effectiveness of the proposed CSCSC strategy is assessed by contrasting its outcomes in two literature-based benchmark issues with those of existing approaches. To determine the greater concert of CSCSC, the effects of the suggested methodology are associated with six methods for extracting the parameters of four different PV models, specifically SDM, DDM and PVM. The numerical experiments validate that the new algorithm performs better than previous techniques in the literature and is capable of delivering superior optimal solutions. The simulation findings demonstrate that the innovative optimization methodology may outperform existing approaches in a variety of solar cells, achieving the lowest RMSE. In order to categorize the parameter in various PV model cells, the suggested CSCSC approach is used. Providing a reliable, accurate and effective parameter estimate is the aim of CSCSC. This novel hybrid approach, which is in line with recent developments in the renewable energy industry, offers improved performance and efficiency for solar PV systems.

The following is a quick description of this paper's primary contributions:

1) A hybrid technique (CSCSC) has been devised for the purpose of identifying parameters in different PV models.

2) In terms of accuracy and stability, CSCSC constantly evaluates its parameter identification of various PV cell models and numerical function to current cutting-edge methodologies.

3) The CSCSC algorithm enhances the exploitation capabilities of both SCO's and CSCO's, potentially leading to substantial improvements in discovery outcomes.

This paper is organized as follows: In Section 2, a novel recommended approach is presented. The difficulty in the PV cell model is defined in Section 3. Section 4 presents the experimental case study and findings. A summary of the research is provided in Section 5.

2. Overview of proposed method

2.1 Sand Cat Optimization (SCO)

The ability of sand cats (SC) to recognize low-frequency noises in their environment is what gives the SCO approach its name.[48] The two highest activities of the SC are hunting and prey assault. The frequency absorption of the SC at frequencies below 2 kHz is astounding, according to scientific studies. At this frequency, house cats are about 8 dB less sensitive than SCs.[50] These distinctive characteristics enable the SC to track prey, detect sound (prey movement), and hunt successfully depending on prey position.

Each issue variable is represented by a SC in the SCO algorithm. The applicant matrix for the SC inhabitants is first produced at random between the lower and upper bounds of the design variables in the SCO technique. As shown in Fig. 1, the size of the applicant matrix for a d-dimensional optimization interplanetary with n SCs is equal to $N_{pop} \times N_d$, where $pop = 1, \ldots, n$.

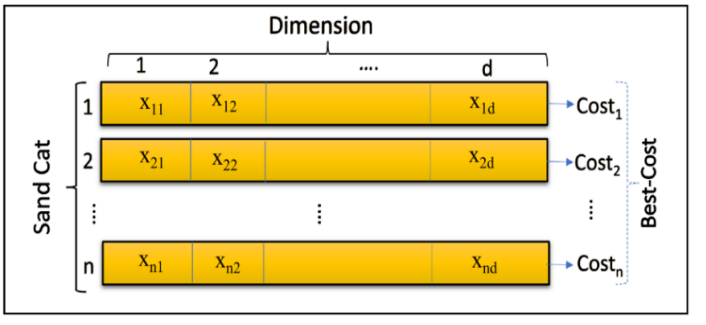

Fig. 1 Creation of the initial candidate matrix.

Additionally, a particular fitness function is calculated to determine each SC's fitness value (*i.e.*, cost). A value for the associated function will be produced by each SC (*i.e.*, candidate solution). The SC with the lowest worth at the end of an iteration is chosen as the most suitable option, and in the subsequent iteration, the several contenders try to go in the direction of this chosen cat. In each cycle, the optimal response can correspond to the cat that is closest to the prey.

The solutions to each SC are denoted by $X_i = (x_{i1}, x_{i2}, \ldots, x_{id})$, $(i = 1, \ldots, n)$. The SCO algorithm makes use of the SC's ability to hear at low frequencies. The SC can sense frequencies lower than 2 kHz, as was before mentioned. As a consequence, it is assumed that a SC's sensitivity range when looking for prey begins at 2 kHz and stops at 0 kHz. The vector $\overrightarrow{r_G}$ is added to represent this mechanism and in the mathematical simulation of the algorithm, and it will linearly decline 0 from two as the amount of iterations grows in accordance with the next equation[48]:

$$\overrightarrow{r_G} = S_M - \left(\frac{S_M \times t}{t_{max}}\right) \quad (1)$$

It is based on the SC's hearing qualities, the S_M value is meant to be 2.[48] The maximum number of iterations is indicated by t_{Max}, where t denotes the present iteration. Each search agent's position is updated throughout the searching phase based on the best-candidate situation ($\overrightarrow{Pos_b}$), its current situation $\overrightarrow{Pos_c}$,

and its sensitivity range ($\vec{r}$), using the following equation:

$$\overrightarrow{Pos}(t+1) = \vec{r}.(\overrightarrow{Pos_b}(t) - rand\ (0,1).\overrightarrow{Pos_c}(t)) \quad (2)$$

Separately SC has a unique sensitivity range ($\vec{r}$), which is determined by Eq. (3), to avoid the local optimum trap.

$$\vec{r} = \overrightarrow{r_G} \times rand\ (0,1) \quad (3)$$

The broad sensitivity range is thus ($\overrightarrow{r_G}$), which is linearly decreased from 2 to 0. Additionally, $\vec{r}$ displays each cat's sensitivity range.[48]

The following equation is used to update each SC's position both after examining and during the attacking phase of SCO:

$$\overrightarrow{Pos}(t+1) = \overrightarrow{Pos_b}(t) \text{-} \vec{r}.\overrightarrow{Pos_{rnd}}.\cos(\theta) \quad (4)$$

where ($\overrightarrow{Pos_{rnd}}$) is the location of a randomly chosen SC based on the next equation, and θ is a random angle among 0 and 360.

$$\overrightarrow{Pos_{rnd}} = \left|rand\ (0,1).\overrightarrow{Pos_b}(t) - \overrightarrow{Pos_c}(t)\right| \quad (5)$$

Lastly, The last and most crucial component of the method for determining when to switch between the exploration (searching) and exploitation (attacking) phases is the R parameter, which is derived from Eq. (6).[48]

$$\vec{R} = 2 \times \overrightarrow{r_G} \times rand\ (0,1) - \overrightarrow{r_G} \quad (6)$$

The SCO militaries the exploration causes to exploit once R is fewer than or equal to 1; otherwise, they are compelled to explore and discover prey.[36] As a result, Eq. (6) serves as the SCO algorithm's final updating position equation.[48]

$$\vec{X}(t+1) = \begin{cases} \overrightarrow{Pos_b}(t) - \overrightarrow{Pos_{rnd}}(t).\cos(\theta).\vec{r} & |R| \le 1; exploitation \\ \vec{r}.(\overrightarrow{Pos_{bc}}(t) - rand\ (0,1).\left(\overrightarrow{Pos_c}(t)\right) & |R| > 1; exploitation \end{cases} \quad (7)$$

as shown by Eq. (7). When $|R| \le 1$, SCs are told to attack their prey; if not, they are instructed to look for another workable option in the region. The SCO pseudocode is found in Algorithm 1.

2.2 CSCO method

The objective of the current study is to demonstrate the worldwide search capacity of the SCO. In order to accomplish this and increase the algorithm's exploring capability, the chaotic series is used in the sensitivity range parameter of Eq. (3).

Unpredictability, irregularity, and stochastic characteristics are characteristics of chaotic processes, which are deterministic organizations modified by the initial conditions. Due to their intrinsic irregularity, chaotic limits can move external of specified bounds without retelling. A chaotic map is one that may produce chaotic movement and exhibits some form of chaotic pattern. The well-known logistic map applied in this study, which is based on the equation:

$$\mu(t+1) = a\ \times\ \mu(t) \times (1 - \mu(t)) \quad (8)$$

where t is the iteration number and , μ (t) denotes the chaotic map. a stands for a constant that is equal to 4. μ(0) should not be identical to 0, 0.25, 0.5, 0.75, or 1. μ (0) should be initialized between 0 and 1. The sensitivity range ($\vec{r}$) evaluation equation in the CSCO uses the μ as a simple random integer to improve the algorithm's stochastic characteristics while avoiding previous convergence. In light of the following equation, a SC's position will be updated:

$$\vec{X}(t+1) = \begin{cases} \overrightarrow{Pos_b}(t) - \overrightarrow{Pos_{rnd}}(t).cos\ (\theta).\overrightarrow{r_G} \times \mu & |R| \le 1; exploitation \\ \overrightarrow{r_G} \times \mu\ .(\overrightarrow{Pos_{bc}}(t) - rand\ (0,1).\left(\overrightarrow{Pos_c}(t)\right) & |R| > 1; exploitation \end{cases} \quad (9)$$

Additionally, in the proposed CSCO, a new SC will be substituted for the weakest SC delivering the greatest fitness value at individually iteration in order to develop the algorithm's exploration and search abilities, as shown in the following equation:

$$x_{worst} = \begin{cases} rand_1 \times \overrightarrow{Pos_{rnd}}(t)\ \ if\ rand_3 \le 0.5 \\ x_{i\,min} + rand_2 \times (x_{i\,max} - x_{i\,min}) \end{cases} \quad (10)$$

where $rand_1$, $rand_2$and $rand_3$ are uniform random numbers between 0 and 1, and x_{worst} is the SC with the greatest fitness value. Fig. 2 shows a flow chart of the proposed method.

2.3 Single Candidate Optimizer (SCO)

SCO only takes into account one potential response in its quest for superior alternatives, in contradiction of the bulk of the presently employed searching algorithms, which depend on a swarm of particles, throughout the period of the total optimization procedure. The proposed technique divides the T_{max} function iterations or evaluations into two phases, with each phase's proposed resolution updating its situation in a unique way. The SCO method combines the single candidate method and the two-phase strategy to produce a single, reliable algorithm. The method, most notably, updates the candidate solution's situation solely based on its information, *i.e.*, its position at the moment, using a unique set of equations. The first stage of SCO ends with the completion of T_1 function evaluations, and the second stage, where $T_1 + T_2 = T_{max}$, begins with T_2 function evaluations.

Throughout the first stage of SCO, the candidate explanation moves to the following positions:

$$x_j = \begin{cases} gbest_j + \left(w\left|gbest_j\right|\right)\ if\ rand_1 < 0.5 \\ gbest_j - \left(w\left|gbest_j\right|\right), \end{cases} \quad (11)$$

where $rand_1$ is an integer uniformly chosen at random between [0, 1]. Weight (w) is defined mathematically as follows:

$$\mathrm{w(t)} = exp^{-\left(\frac{bt}{T_{max}}\right)^b} \quad (12)$$

where T_{max} is the maximum number of function evaluations, b is a constant value, and t is the current function evaluation or iteration. The second phase of SCO conducts a deep search after carefully surveying the vicinity of the best place identified in the first phase. The latter parts of Phase Two help to focus on promising regions and restrict the search area. The candidate solution shifts into a new place as the second phase goes on, as seen below:

$$x_j = \begin{cases} gbest_j + w \times rand_2(ub_j - lb_j) & if\ rand_2 < 0.5 \\ gbest_j - w \times rand_2(ub_j - lb_j) & else \end{cases} \quad (13)$$

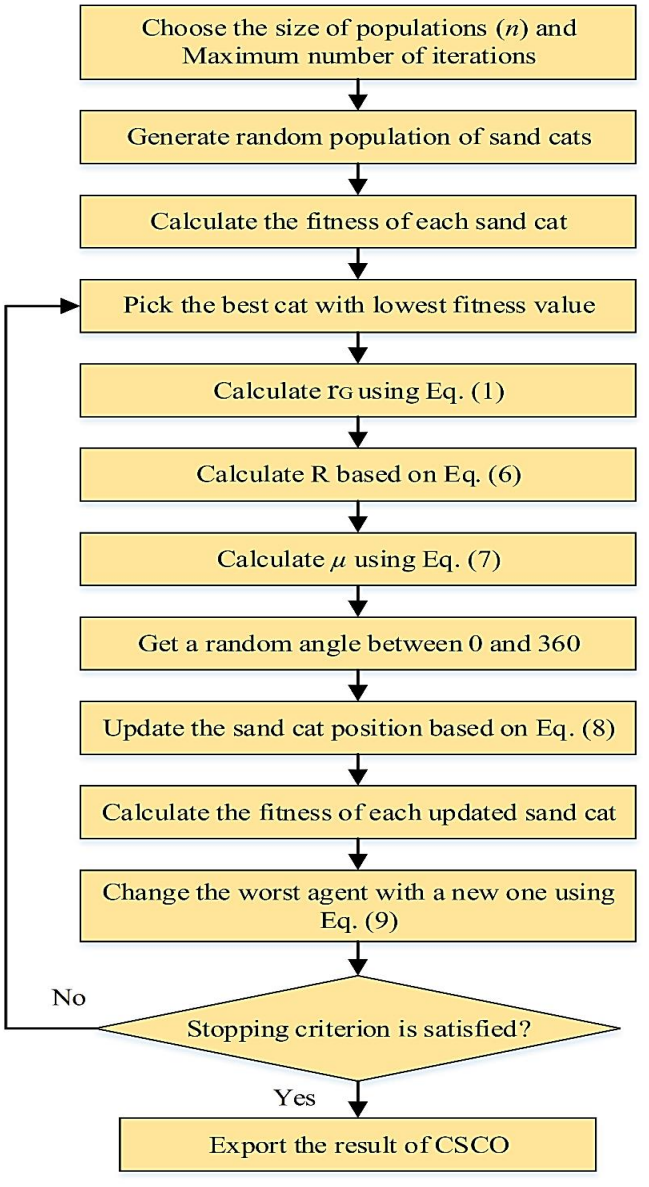

Fig. 2 Algorithm for CSCO.

where ub_j and lb_j are the upper and lower bounds of the boundaries, and $rand_2$ is a separate random mutable with a [0, 1] variety. The most important SCO parameter, w, is in responsible of finding the right stability among exploration and exploitation. The amount of function assessments leads to an exponential decline in w from Eq. (12). A comparatively large value of w at the start of the search procedure helps in efficiently exploring the search space, while a small value of w at the end of the optimization method increases the exploitation capabilities. This behavior is crucial. One of the major problems of MA approaches is their propensity to become caught in local optima, especially in the later phases of the search process. The second step of SCO's solution to this issue involves revising the position of the candidate solution in a different manner if no fitness improvement is seen after m successive function evaluations. A counter c is used to determine the number of function evaluations m that cannot sequentially improve fitness. The binary parameter p, where $p = 1$ denotes an effective fitness enhancement and $p = 0$ shows a failed fitness development, is used to evaluate the updated candidate's potential to realize an effective fitness.

In the next stage of SCO, an applicant solution updates its location in accordance with Eq. (13), but if acting m repeated function assessments does not raise the fitness value, the candidate explanation relocates as follows:

$$x_j = \begin{cases} gbest_j + rand_3(ub_j - lb_j) & if\ rand_2 < 0.5 \\ gbest_j - rand_3(ub_j - lb_j) & else \end{cases} \quad (14)$$

In Eq. (14), the candidate solution can change from exploitation to exploration, which aids in its emission from the local minimum. It is infrequently possible for the values of some variables to diverge from the intended range or boundaries when their placements are altered. The updated locations are set as follows to stop a variable from crossing its upper bound or lower bound if the value of the variable is larger than either.

$$x_j = \begin{cases} gbest_j & if\ x_j > ub_j \\ gbest_j & if\ xj < lb_j \end{cases} \quad (15)$$

In Eq. (15), the efficient measurement of an applicant solution is allocated the same value as the overall best value if the efficient position is outside the bounds. In SCO, one candidate solution x is randomly generated and then iteratively updated to search for a superior one. Fig. 3 shows the flowchart for the SCO. The creation of the first possible solution is shown below.

$$x_j = lb_j + rand_4(ub_j - lb_j) \quad (16)$$

2.4 Hybrid CSCO and SCO

A hybrid approach to problem solving combines two or more methodologies to address the same concern. The goal of hybridization is to combine the advantages of each strategy to improve the outcome's accuracy.[51] The CSCO and SCO approaches have been combined to create the CSCSC methodology, which has been created in the current study. The proposed method, a global optimization technique, successfully searches the problem space and is likely to yield an optimal or nearly optimal result. Therefore, it may be utilized in conjunction with local optimization methods like SCO.

The SCO is useful for analyzing a small area, but it is rarely useful for analyzing larger regions. The proposed hybrid technique may combine the enormous global and local searching capabilities of the SCO algorithm and those of the CSCO. The global performance of CSCO is excellent, while local minima are easily evaded. The CSCO can improve the accuracy of the findings by increasing the number of iterations. When there are enough generations, CSCO can increase the findings' accuracy, but not before. CSCO's local search functionality is still lacking as a result.

The start point has an important impact on the results of the SCO since it uses a local optimization strategy. However, SCO will be a simple and effective strategy if a great starting point is chosen. we successfully combine the benefits of SCO as a

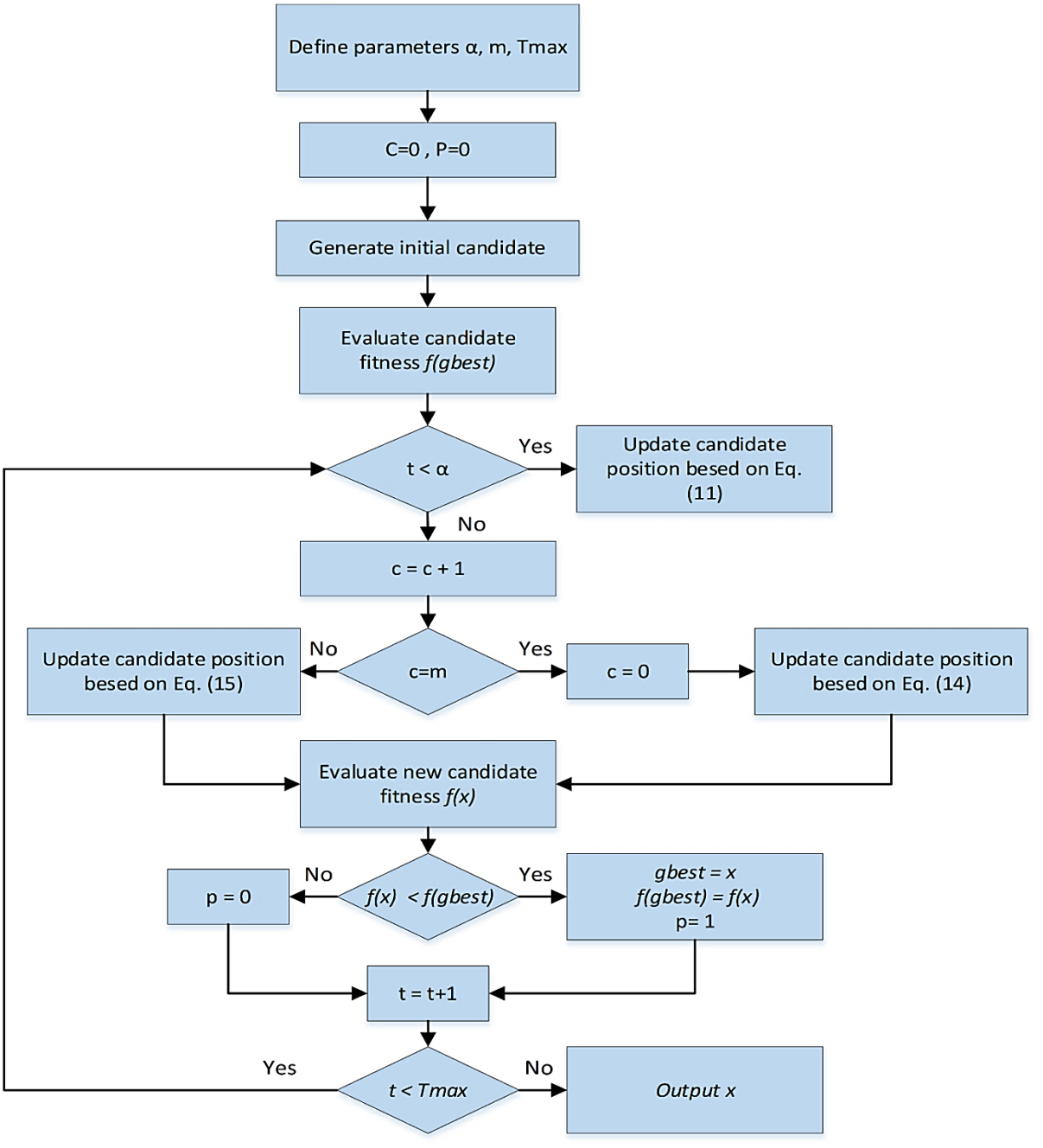

Fig. 3 Flowchart for the SCO.

local optimization and CSCO as a global optimization to discover the best solution. Since the SCO depends on the first solution, the hybrid strategy that has been proposed starts with the CSCO.

The CSCO is hired to keep watch after a specific number of repeats. The SCO is then given the go-ahead to conduct a local search beginning with the CSCO's top choice. It is important to note that picking the appropriate initial point will increase the method's stability while also increasing the accuracy of the outcomes. The SCO studies a random solution to be the starting point in the absence of any knowledge. The method is unable to locate the overall best and becomes less stable if this random answer is extremely distant from the global optimal solution. Fig. 4 shows the procedure flow of the recommended hybrid CSCSC.

3. Problem definition

Scholars have extensively researched equivalent circuit models to uncover the PV cell's critical unknown properties. The I-V characteristics are illustrated using four models, and the associated objective function (OF) is displayed in this section. The analogous circuit diagram for the SDM, DDM and PVM models is shown in Fig. 5.[19,52]

3.1 SDM

As seen in Fig. 5(a), the SDM, which is popular and suitable for addressing PV cell static characteristics, has been used by many researchers to understand the key needs of solar PV

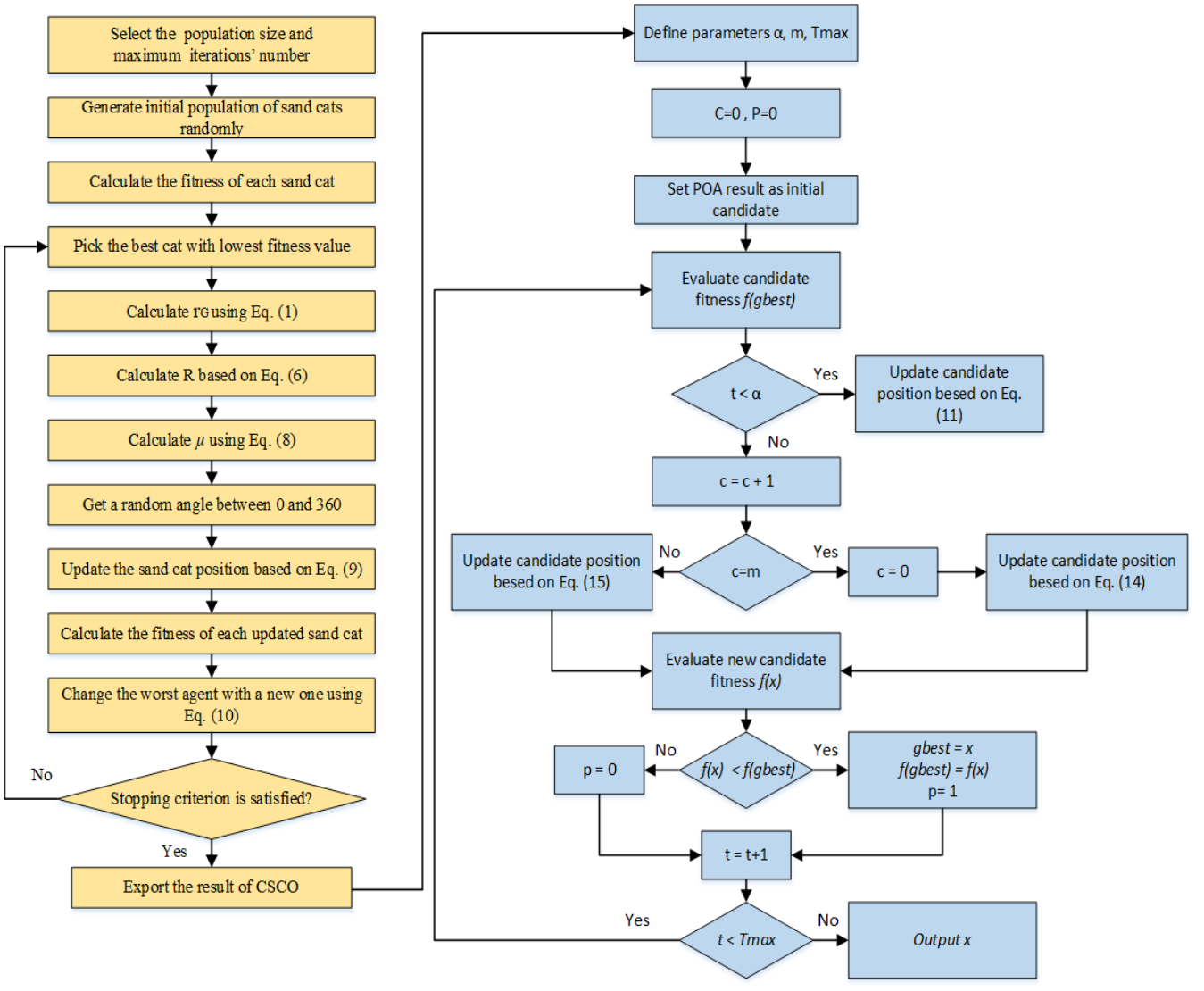

Fig. 4 Hybrid CSCSC.

models. A diode, a constant current source (I_{ph}), a series resistor (R_s), and a parallel resistor (R_{sh}) are main components of this model. When current passes via a diode, the PV model output formula is governed by Eq. (17).[52,53]

$$I_L = I_{Ph} - I_{sd}\left(exp\left(\frac{q(V_L+R_sI_L)}{nkT}\right)-1\right)-\frac{(V_L+R_sI_L)}{R_{sh}} \quad (17)$$

where I_{sd} is the reverse saturate current. The PV voltage is v_L; the charge for the electron is q; the diode ideal factor is n; the Boltzmann constant is k; and the test temperature is T. To summarize, the SDM has five unknown parameters as follows:

$$X = \{I_{ph}, I_{sd}, R_s, I_{sh}, n\}$$

3.2 DDM

According to Fig. 5(b), the DDM model, which contains two diodes in parallel with the current source, can more closely describe the properties of PV cells in a hard environment than the SDM model.[54] The output current of DDM (I_{ph}) is

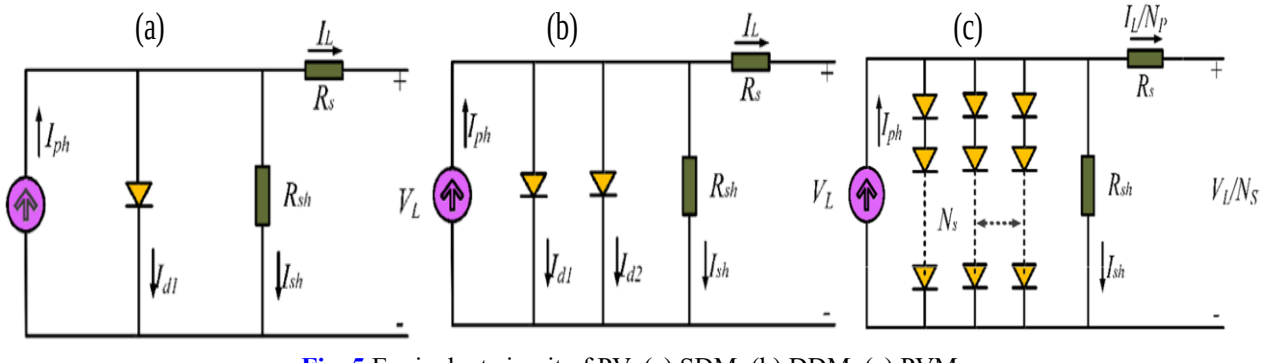

Fig. 5 Equivalent circuit of PV: (a) SDM, (b) DDM, (c) PVM.

depended on the current flowing across the two diodes as follows:

$$I_L = I_{Ph} - I_{sd1}\left(exp\left(\frac{q(V_L + R_s I_L)}{n_1 kT}\right) - 1\right) - I_{sd2}\left(exp\left(\frac{q(V_L+R_s I_L)}{n_2 kT}\right) - 1\right) - \frac{(V_L+R_s I_L)}{R_{sh}} \quad (18)$$

where n_1 and n_2 are the ideality factors for the diffusion and recombination diodes, respectively, and I_{sd1} stands for the diffusion current and I_{sd2} for the saturation current. $X = \{I_{ph}, I_{sd1}, I_{sd2}, R_s, I_{sh}, n_1, n_2\}$ are seven characteristics of the DDM that need to be accurately identified.

3.4 PVM

Many diodes are coupled in series and parallel to make up the PVM, illustrated in Fig. 5(d). Its I-V connection's mathematical model is described below.[52,55]

$$I_L = I_{Ph}N_P - I_{sd}N_P\left(exp\left(\frac{V_L+R_s I_L N_s/N_p}{nN_s\frac{kT}{a}}\right) - 1\right) - \frac{V_L+R_s I_L N_s/N_p}{R_{sh}N_s/N_p} \quad (19)$$

where N_p and N_s are the parallel and series numbers of solar cells, respectively. The 5 unknown parameters for the extraction of the PVM are $X = \{I_{ph}, I_{sd}, R_s, I_{sh}, n\}$.

3.5 Problem formulation

These models are the most typical ones. In order for an optimization method to determine exact parameter values, the equations are converted into related optimization difficulties. The Objective Function (OF) shows the least difference among the estimated and experimental data when the ideal parameter values are used. The majority of algorithms, according to [53], employ the total RMSE as their assessment criterion. The RMSE may also be used to assess the disparity between predicted and actual results. So, RMSE is nominated as the OF:

$$OF(X) = RMSE(X) = \sqrt{\frac{1}{M}\sum_{d=1}^{M} f(V_L, I_L, X)^2} \quad (20)$$

where X stands for the vector holding the to be estimated unknown parameters and M is the total number of experimental I-V data points. The error function (f) is defined for different PV models as follows:

• For SDM:

$$\begin{cases} f(V_L.I_L.\boldsymbol{X}) = I_{ph} - I_{sd}\left(exp\left(\frac{q(V_L+R_s I_L)}{nkT}\right) - 1\right) - \frac{V_L+R_s I_L}{R_{sh}} - I_L \\ \boldsymbol{X} = \{I_{ph}.I_{sd}.R_s.R_{sh}.n\} \end{cases} \quad (21)$$

• For DDM:

$$\begin{cases} f(V_L.I_L.\boldsymbol{X}) = I_{ph} - I_{sd1}\left(exp\left(\frac{q(V_L+R_s I_L)}{n_1 kT}\right) - 1\right) \\ -I_{sd2}\left(exp\left(\frac{q(V_L+R_s I_L)}{n_2 kT}\right) - 1\right) - \frac{V_L+R_s I_L}{R_{sh}} - I_L \\ \boldsymbol{X} = \{I_{ph}.I_{sd1}.I_{sd2}.R_s.R_{sh}.n_1.n_2\} \end{cases} \quad (22)$$

• For PVM:

$$\begin{cases} f(V_L.I_L.\boldsymbol{X}) = I_{ph}N_p - I_{sd}N_p\left(exp\left(\frac{V_L+R_s I_L N_s/N_p}{nN_s\frac{kT}{q}}\right) - 1\right) \\ -\frac{V_L+R_s I_L N_s/N_p}{R_{sh}N_s/N_p} \\ \boldsymbol{X} = \{I_{ph}.I_{sd}.R_s.R_{sh}.n\} \end{cases} \quad (23)$$

4. Numerical experiments and comparisons

The following subsections will present and compare the results produced from the proposed algorithm for numerical function optimization and PV parameters with other MA approaches. This comparison aims to assess the efficacy of the suggested method.

4.1 Evaluation of CSCSC on benchmark tests

This section compares and confirms the performance of the CSCSC with a set of numerical benchmark test.[27,56] Table 1 expressed various mathematical functions along with their properties for benchmarking optimization methods. Fig. 6 provide three-dimensional illustrations of these functions.

Typical conventional functions are divided into two types: multi-modal with multiple local minimums and a global model. Multi-modal functions can evaluate algorithms' capacity to escape local optima and achieve exploratory investigation, while unimodal functions with a single global finest can determine algorithms' speed and capability to dominate. The

Table 1. Explanation of unimodal purposes.

Function	Name	Range	f_{min}	Dim
$F_1(X) = \sum_{i=1}^{n} x_i^2$	Sphere function	$[-100, 100]^n$	0	30
$F_2(X) = \sum_{i=1}^{n} \lvert x_i \rvert + \prod_{i=1}^{n} \lvert x_i \rvert$	Schwefel problem 2.22	$[-10, 10]^n$	0	30
$F_3(X) = \sum_{i=1}^{n} \left(\sum_{j=1}^{i} x_j\right)^2$	Schwefel problem 1.2	$[-100, 100]^n$	0	30
$F_4(X) = \max_i\{\lvert x_i \rvert, 1 \le i \le n\}$	Schwefel problem 2.21	$[-30, 30]^n$	0	30
$F_5(X) = \sum_{i=1}^{n-1} [100(x_{i+1} - x_i^2)^2 + (x_i - 1)^2]$	Gernalized Rosenbrock function	$[-100, 100]^n$	0	30
$F_6(X) = \sum_{i=1}^{n} ([x_i + 0.5])^2$	Step function	$[-100, 100]^n$	0	30
$F_6(X) = \sum_{i=1}^{n} i x_i^4 + \boldsymbol{random}[\boldsymbol{0}, \boldsymbol{1}]$	Quartic function with noise	$[-1.28, 1.28]^n$	0	30

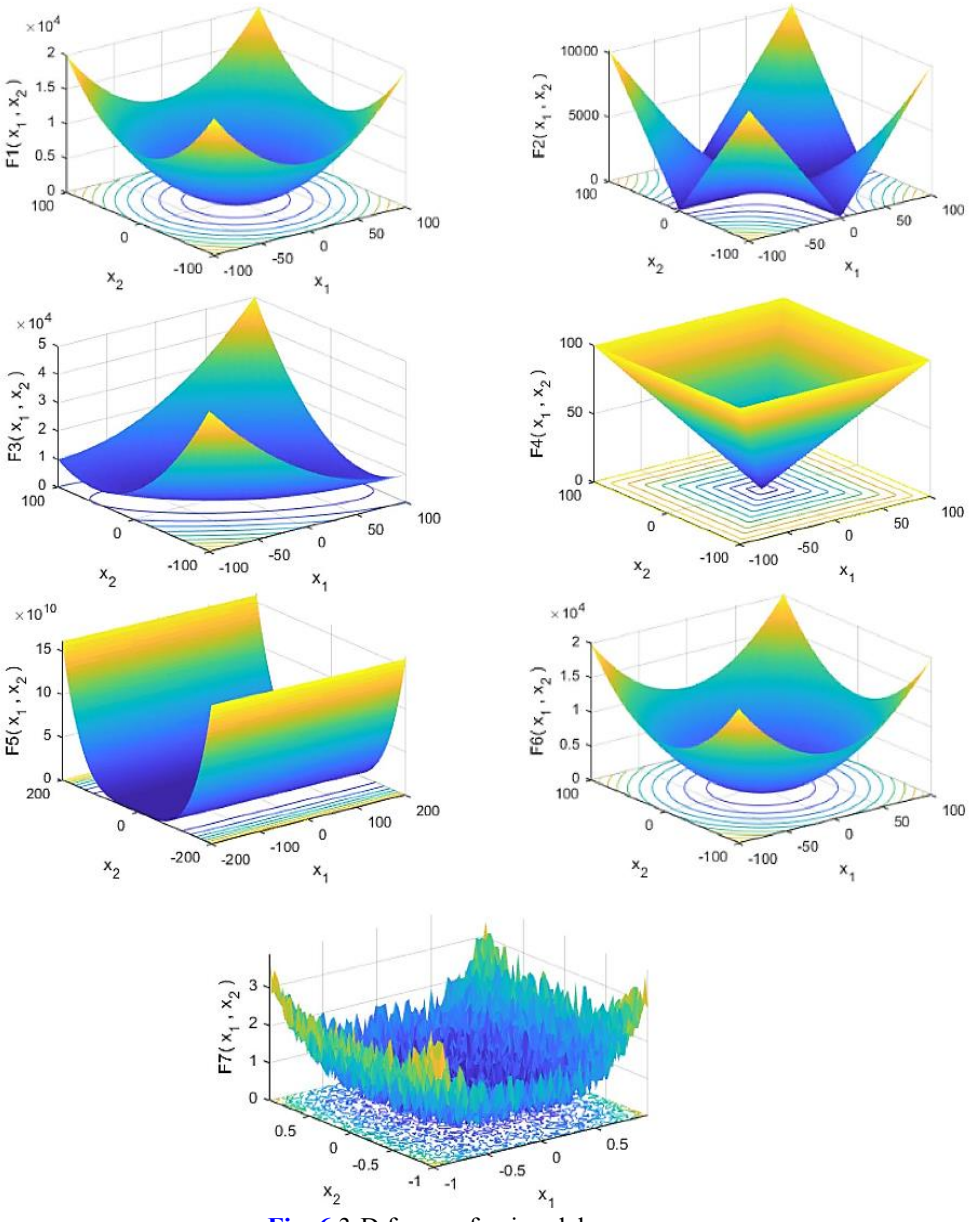

Fig. 6 3-D forms of unimodal purposes.

suggested algorithmic techniques were generated in MATLAB R2020b. Also, all functions have a fixed dimension of 30.

The original SCO and the proposed CSCSC are compared against various MAs techniques including PSO,[39] IJAYA,[40] MVO,[28] TSA[27] and SSA.[43] In order to compare all techniques fairly, the amount of explanations (N) and the maximum number of iterations (t_{max}) of each set are kept at 30 and 1000, respectively. Due to randomness characteristics of MA techniques, outcomes of a single run are unpredictable and may not be accurate. Therefore, numerical examination should be approved out so that give a reasonable evaluation and evaluate the success of the algorithms. The findings of 30 iterations of the aforementioned procedures are used to remedy this issue.

Table 2 determine that, for all purposes, CSCSC may agreement greater solutions than traditional SCO as well as other optimization strategies in terms of the mean value of the OFs. The effects also establish that the CSCSC algorithm's mean and standard deviation are significantly lesser than those of the other procedures, representing the algorithm's immovability. The outcomes show that CSCSC strokes both the conventional technique and other optimization approaches.

4.2 Evaluation of CSCSC on PV models

This section conducts a number of tests on four PV models to estimate the efficiency of the suggested CSCSC for parameter valuation. The SDM, DDM and polycrystalline Photowatt-PWP201 modules are the four kinds in question. these values are calculated using a 57 mm diameter commercial silicon R.T.C France solar cell at 33 °C and 1000 W/m^2 [10]. Searches for the best approximation of This work introduces the Photowatt-PWP201 PVM, which has 36 connected cells arranged in series operating at 45 °C.[57,58] The parameter search choices for the PV models are displayed in Table

Table 2. Evaluation of different MA methods in resolving unimodal purposes.

F	Index	CSCSC	CSCO	PSO	IJAYA	TSA	SSA	MVO
F_1	Mean	0.000	2.42×10^{-97}	4.78×10^{-09}	0.0071	0.2810	$3.29E^{-07}$	8.31×10^{-56}
	Std.	0.000	7.22×10^{-97}	1.60×10^{-08}	0.0032	0.1110	$5.92E^{-07}$	1.02×10^{-58}
F_2	Mean	0.000	1.16×10^{-52}	0.0006	0.4340	0.3960	1.9111	8.36×10^{-35}
	Std.	0.000	2.55×10^{-52}	0.0028	0.1840	0.1410	1.6142	9.86×10^{-35}
F_3	Mean	4.37×10^{-178}	7.84×10^{-81}	18.700	1660.0	43.100	1500.0	1.51×10^{-14}
	Std.	5.76×10^{-181}	3.49×10^{-80}	4.4300	672.00	8.9700	707.05	6.55×10^{-14}
F_4	Mean	2.58×10^{-106}	4.5×10^{-46}	0.7100	0.1110	0.8800	2.44×10^{-05}	1.95×10^{-05}
	Std.	4.49×10^{-108}	9.98×10^{-46}	0.3670	0.0475	0.2500	1.89×10^{-05}	0.0004
F_5	Mean	0.271	28.000	57.800	79.700	118.00	136.56	28.400
	Std.	0.568	0.8730	40.900	73.900	143.00	154.00	0.8420
F_6	Mean	4.77×10^{-07}	2.1500	0.7760	0.0069	0.0202	5.72×10^{-07}	3.6700
	Std.	2.25×10^{-07}	0.4470	0.0298	0.0036	0.0074	2.44×10^{-07}	0.3353
F_7	Mean	3.73×10^{-06}	0.0002	0.0894	0.6620	0.0524	8.82×10^{-05}	0.0018
	Std.	3.36×10^{-06}	0.0001	0.0206	0.4200	0.0137	6.94×10^{-05}	0.0004

3.[40,59,60]. As can be seen, the method calculates the errors between the observed and estimated currents for each iteration, and then uses Eq. (20) to determine the RMSE. The CSCSC algorithm's goal is to reduce the quantity of obtained RMSE. Six algorithms were competing against CSCSC: SCO, TSA, SSA, PSO, MVO, and IJAYA. The same experimental parameters were used for the development of all algorithms. Each algorithm was run separately 30 times in this experiment, yielding a total of 30 answers for all the methods that were existence associated. 20000 function evaluations were the maximum allowed. The highest number (*Max*), the lowest number (*Min*), the average number (*Mean*), and the standard deviation (*std*) were used to calculate the RMSE of the algorithms in the simulated experiment.

Table 3. The PV models' parameter settings.

Parameters	PWP201		RTC. France	
	Min	*Max*	*Min*	*Max*
I_{ph} (A)	0	2	0	1
I_{sd} (μA)	0	50	0	1
I_{sd1} (μA)	0	50	0	1
I_{sd2} (μA)	0	50	0	1
I_{sd3} (μA)	0	50	0	1
R_s(Ω)	0	2	0	0.5
R_{sh}(Ω)	0	2000	0	100
n	1	50	1	2
n_1, n_2, n_3	1	50	1	2

4.2.1 Results of the SDM

The minimal standards of the four displays are bolded in Table 4 below, which displays the *Max, Min, mean*, and *Std* of RMSE for CSCSC, SCO, TSA, SSA, PSO, MVO, and IJAYA. It therefore proves that CSCSC generates a lower RMSE than the other examined methods. The parameter values for SDM obtained using different connected approaches are presented in Table 5. Fig. 7 shows how dependable CSCSC is. Both the computed data and the experimental current and voltage data are shown as dots in Fig. 7a. The trend of actual and estimated data on power as it fluctuates with voltage is shown in Fig. 7b. The absolute error (*IAE*) of the measured current as the voltage rises is shown in Fig. 7c. The *RE* trend is shown in Fig. 7d. The total imprecision of power as voltage rises is seen in Fig. 7e. The relationship among voltage and relative power error is shown in Fig. 7f. The test's findings indicate that the outcome will be better the lower the *IAE* inaccuracy. Experimental data from CSCSC is more comparable to actual data. In brief, CSCSC achieves superior than other methods for classifying unknown the parameters.

4.2.2 Results of the DDM

The results of the *Max, Min, Mean*, and *Std*. RMSE indicators are shown in Table 6. The difference between the simulated and measured data is proportional to the RMSE value. This leads us to believe that CSCSC can predict unknown DDM parameters with reasonable accuracy. The parameters obtained through different methodologies are also included in Table 7. Obviously, Indicating that the expected value and experimental value are most closely connected, CSCSC has the lowest RMSE. Additionally provided are the outcomes of the RSME and the Wilcoxon rank test. The results of the study indicate that the CSCSC algorithm demonstrates superior performance compared to other algorithms of similar nature. Fig. 8 shows how the simulation's results turned out. The measurement trend lines for current and voltage are also shown in Fig. 8a. Fig. 8b displays the experimental results of power changing with voltage measurement. The IAE of recorded current as it fluctuates with measured voltage is shown in Fig. 8c. Fig. 8d illustrates the RE changing with the voltage measurement. The IAE of power as a function of voltage is shown in Fig. 8e. The connection among RE and power and voltage are seen in Fig. 8f. The figures demonstrate how well CSCSC mimics the real data and demonstrates the possibility of parameter detection on DDM.

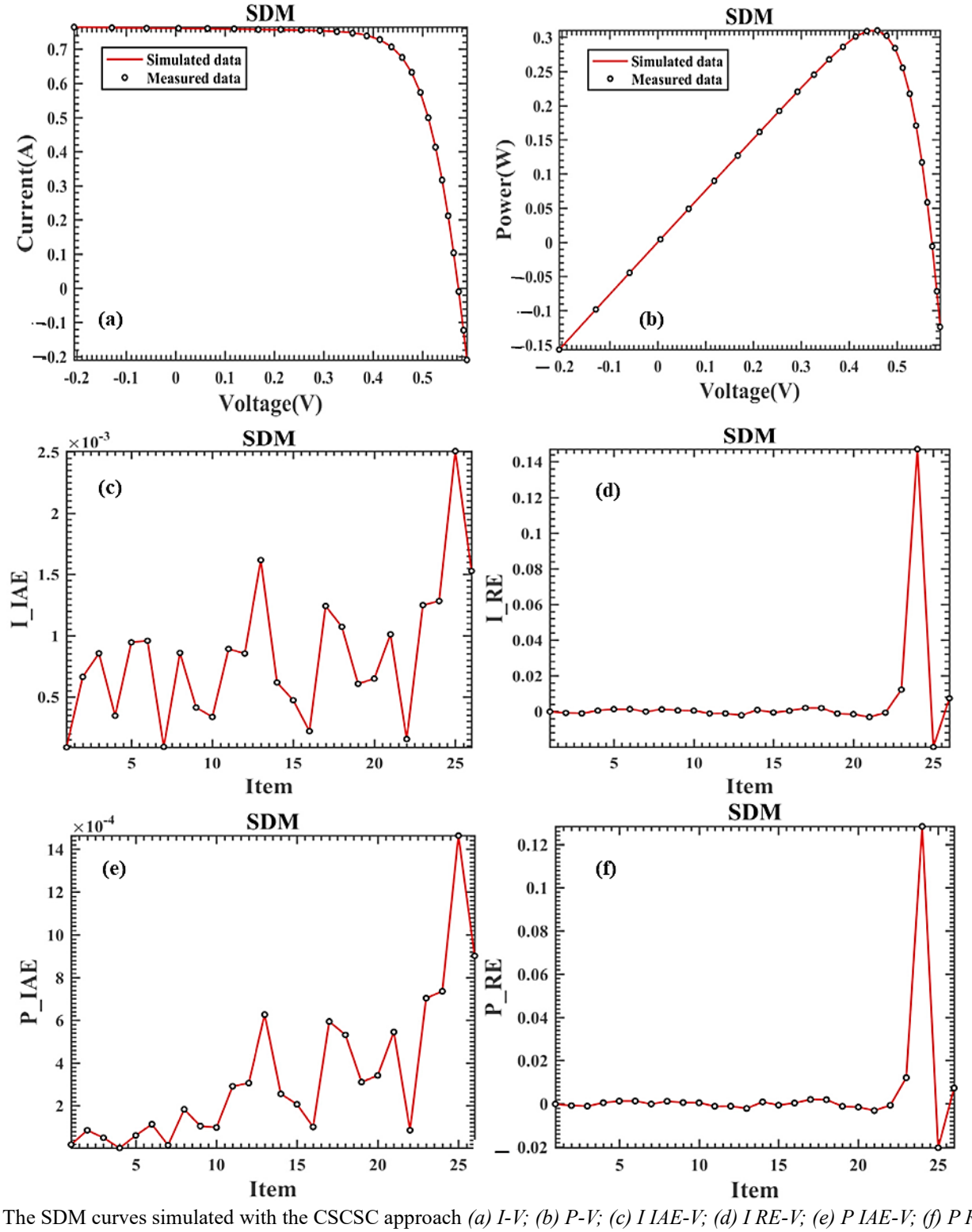

Fig. 7 The SDM curves simulated with the CSCSC approach *(a) I-V; (b) P-V; (c) I IAE-V; (d) I RE-V; (e) P IAE-V; (f) P RE-V.*

Table 4. The statistical findings of the algorithms' RMSE.

Algorithm	*Max*	*Min*	*Mean*	*Std*
CSCPS	0.000986026	0.000986022	0.000986023	1.12316×10^{-9}
SCO	0.001565142	0.000988512	0.001197503	0.000150923
PSO	0.001674660	0.000986168	0.001086513	0.000125814
IJAYA	0.002356831	0.001027920	0.002377086	0.000170656
TSA	0.001560495	0.000990501	0.001086508	0.000125814
SSA	0.013157701	0.001638823	0.003669025	0.002714397
MVO	0.001833410	0.001027901	0.001349724	0.000191389

Table 5. Calculated parameters and RMSE value.

Method	I_{ph} (A)	I_{sd} (A)	R_s (Ω)	R_{sh} (Ω)	n	RMSE	Sig
CSCPS	0.760775	3.2302×10^{-7}	0.036371	53785	1.4818	**0.000986021**	~
SCO	0.760776	3.2297×10^{-7}	0.036375	53.701	1.4817	0.000988767	+
PSO	0.760775	3.2302×10^{-7}	0.036781	53.786	1.4818	0.000986126	+
IJAYA	0.760980	3.3131×10^{-7}	0.036252	49.135	1.4808	0.001027990	+
TSA	0.770684	7.7808×10^{-7}	0.036853	30.420	1.5704	0.000990726	+
SSA	0.7.0833	3.1602×10^{-7}	0.036476	53.028	1.4798	0.001638820	+
MVO	0.760776	3.1952×10^{-7}	0.036449	53.437	1.4809	0.001027870	+

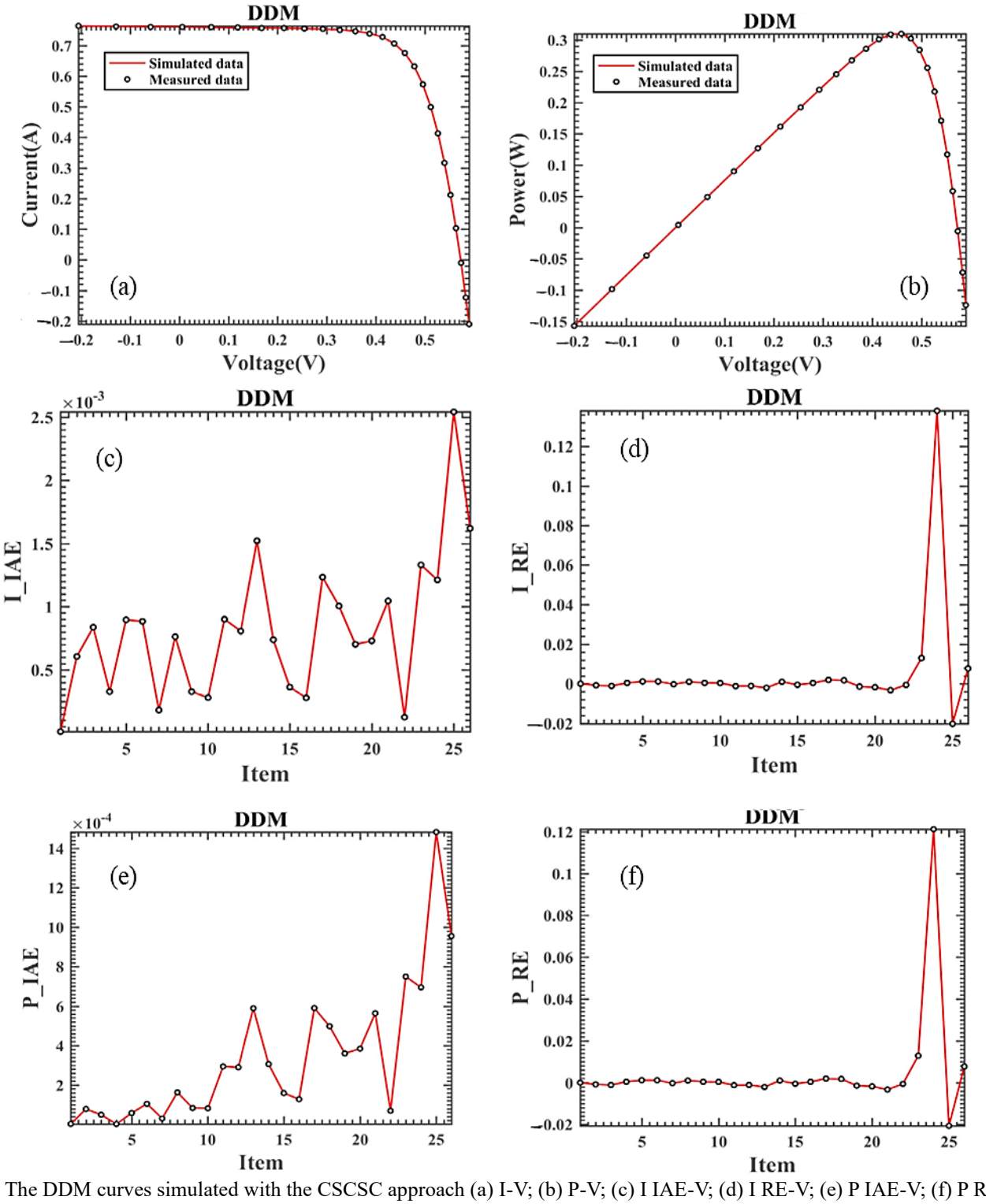

Fig. 8 The DDM curves simulated with the CSCSC approach (a) I-V; (b) P-V; (c) I IAE-V; (d) I RE-V; (e) P IAE-V; (f) P RE-V.

Table 6. The statistical findings of the algorithms' RMSE.

Algorithm	Max	Min	Mean	Std
CSCPS	0.00098775	0.00098350	0.00098625	1.28017×10^{-6}
SCO	0.00243158	0.00098546	0.00153577	0.00041571
PSO	0.00931141	0.00173608	0.00425210	0.00231125
IJAYA	0.00194383	0.00098353	0.00113956	0.00017869
TSA	0.00248306	0.00106254	0.00147935	0.00030199
SSA	0.00186860	0.00098940	0.00115083	0.00018865
MVO	0.00179227	0.00098383	0.00105121	0.00019053

Table 7. Calculated parameters and RMSE value.

Algorithm	I_{ph} (A)	I_{sd1} (A)	R_s (Ω)	R_{sh} (Ω)	n_1	I_{sd2} (A)	n_2	*RSME*	*Sig*
CSCPS	0.761781	6.9944×10^{-7}	0.036715	55.370	1.9999	2.3182×10^{-7}	1.4535	0.000982508	~
SCO	0.76147	3.4274×10^{-7}	0.037050	58.052	1.9101	2.3812×10^{-7}	1.4546	0.000985467	+
PSO	0.71684	1.0000×10^{-6}	0.036840	84.676	2.0000	5.8794×10^{-7}	1.5439	0.001736080	+
IJAYA	0.76083	2.1636×10^{-7}	0.036828	54.557	1.4475	6.4258×10^{-7}	1.9525	0.000983532	+
TSA	0.76084	6.5759×10^{-7}	0.033321	84.745	1.5563	1.8922×10^{-10}	1.8273	0.001062540	+
SSA	0.76083	5.7427×10^{-7}	0.036739	55.185	1.9097	2.1647×10^{-7}	1.4435	0.000989404	+
MVO	0.76030	2.5315×10^{-7}	0.036842	53.800	1.4654	6.9214×10^{-8}	1.6940	0.000983832	+

4.2.4 Results of the PVM

Five elements must be determined for the PVM model. The experiment's RMSE results are presented in Table 8. The experiment was conducted using 1000 W/m^2 and 45 °C. For CSCSC, SCO, TSA, SSA, PSO, MVO, and IJAYA, Table 9 shows four RMSE values: *Max, Min, Mean*, and *Std*. In comparison to other optimizers, CSCSC reaches the best RMSE and the lowest. It is evident that CSCSC demonstrates superior performance compared to the other algorithms that were studied. Numerous PV system metrics assessed by the CSCSC are shown in Fig. 9. The current and voltage measurement trend line is shown in Fig. 9a. When the voltage is monitored, as shown in Fig. 9b, the power data increases. Fig. 9c shows how the measured current becomes increasingly inaccurate as the voltage measurement rises. The relation correctness of current as it fluctuates with voltage measurement is shown in Fig. 9d. Fig. 9e illustrates the complete inaccuracy of the power range derived from voltage measurement. Fig. 9f describes the association among RE, power, and voltage. The graph demonstrates how well the anticipated data and the actual data match. The curve also shows how CSCSC performed better. In terms of parameter identification in the PVM model, CSCSC offers a lot of potential.

This part provides a comprehensive comparison of the preceding techniques, and it offers the opportunity to derive inferences from the statistical findings shown in Table 10. The CSCSC technique has superior performance compared to the other six algorithms in terms of model reliability and average accuracy, as evidenced by the results presented in Table 10.

Table 8. The statistical findings of the algorithms' RMSE.

Algorithm	Max	Min	Avg	Std
CSCPS	0.003003	0.0024250	0.004443	0.000156
SCO	0.274252	0.002.545	0.022052	0.068587
PSO	0.784692	0.153828	0.538447	0.194014
IJAYA	9.201350	0.134059	1.751140	2.290422
TSA	0.002895	0.002457	0.002585	0.000113
SSA	0.003248	0.002426	0.002525	0.000210
MVO	0.004920	0.002626	0.002605	0.000477

Table 9. Calculated parameters and RMSE value.

Algorithm	I_{ph} (A)	I_{sd} (A)	R_s (Ω)	R_{sh} (Ω)	*n*	*RSME*	*Sig*
CSCPS	1.03051	3.48226×10^{-06}	1.20127	981.982	48.6428	**0.002425**	~
SCO	1.03244	3.22121×10^{-06}	1.20226	743.828	48.3583	0.002545	+
PSO	0.95809	9.98267×10^{-07}	1.28797	338.399	45.6897	0.153828	+
IJAYA	1.10436	8.10310×10^{-07}	1.10635	518.714	44.0400	0.134059	+
TSA	1.03181	3.25189×10^{-06}	1.20458	828.997	48.3862	0.002457	+
SSA	1.03073	3.37754×10^{-06}	1.20464	948.448	48.5263	0.002425	+
MVO	1.03070	3.37890×10^{-06}	1.20440	951.290	48.5280	0.002628	+

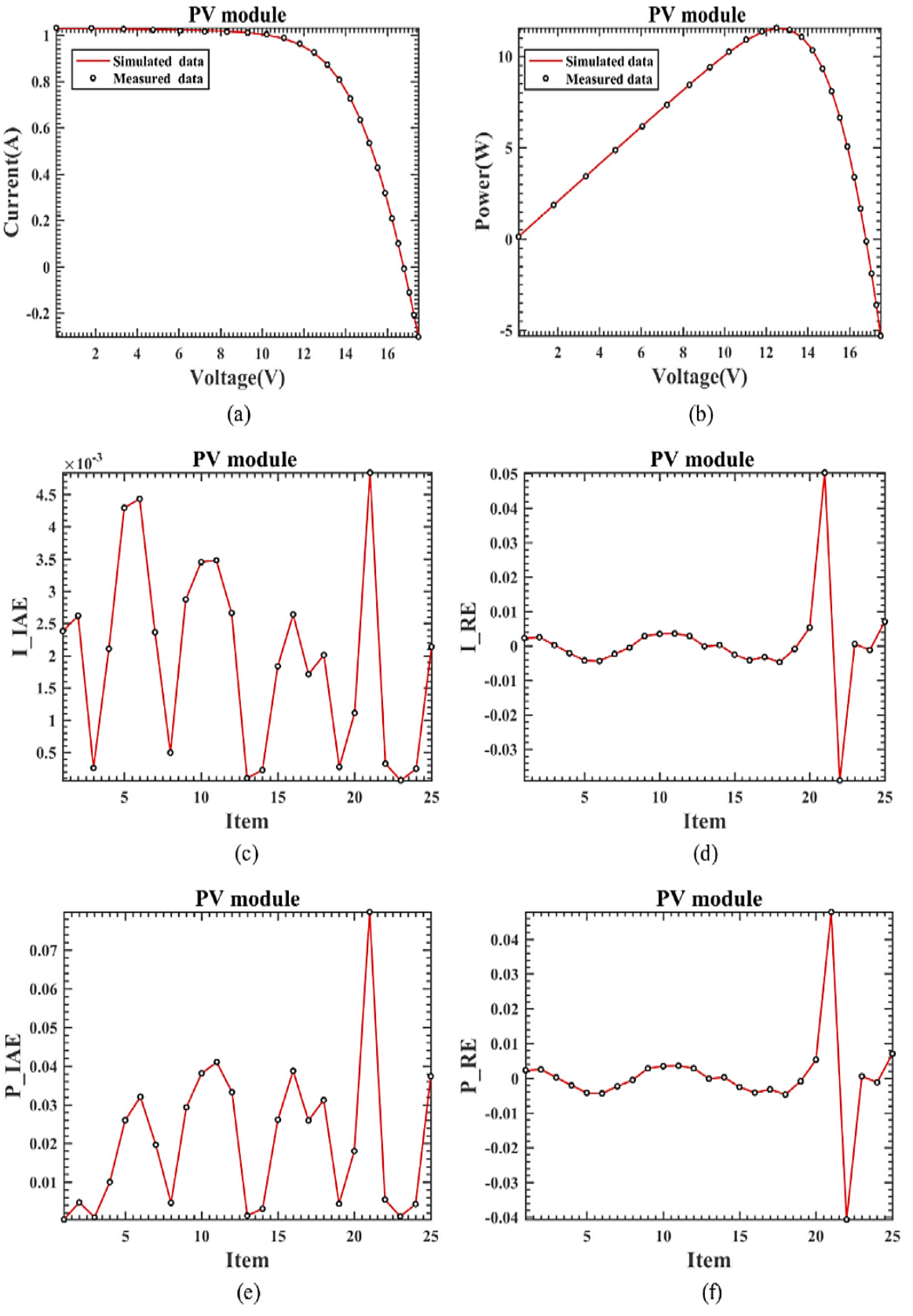

Fig. 9 The PVM curves simulated with the CSCSC approach (a) I-V; (b) P-V; (c) I IAE-V; (d) I RE-V; (e) P IAE-V; (f) P RE-V.

Table 10 demonstrates that the suggested approach has a reduced mean and *Std* in comparison to other available solutions.

5. Conclusions

The present study introduces a novel hybrid optimization methodology, denoted as CSCSC, which integrates the chaotic cat sand optimizer (CSCO) algorithm with the Single

Table 10. Statistical comparison of RMSE values achieved by the tested algorithms for four models.

method		PV models		
		SDM	DDM	PVM
	CSCPS	0.000986026	0.00098775	0.003003
	SCO	0.001565142	0.00243158	0.274252
	PSO	0.001674660	0.00931141	0.784692
Max	IJAYA	0.002356831	0.00194383	9.201350
	TSA	0.001560495	0.00248306	0.002895
	SSA	0.013157701	0.00186860	0.003248
	MVO	0.001833410	0.00179227	0.004920
	CSCPS	0.000986022	0.00098350	0.0024250
	SCO	0.000988512	0.00098546	0.002.545
	PSO	0.000986168	0.00173608	0.153828
Min	IJAYA	0.001027920	0.00098353	0.134059
	TSA	0.000990501	0.00106254	0.002457
	SSA	0.001638823	0.00098940	0.002426
	MVO	0.001027901	0.00098383	0.002626
	CSCPS	0.000986023	0.00098625	0.004443
	SCO	0.001197503	0.00153577	0.022052
	PSO	0.001086513	0.00425210	0.538447
Mean	IJAYA	0.002377086	0.00113956	1.751140
	TSA	0.001086508	0.00147935	0.002585
	SSA	0.003669025	0.00115083	0.002525
	MVO	0.001349724	0.00105121	0.002605
	CSCPS	1.12316×10^{-9}	1.28017×10^{-6}	0.000156
	SCO	0.000150923	0.00041571	0.068587
	PSO	0.000125814	0.00231125	0.194014
Std	IJAYA	0.000170656	0.00017869	2.290422
	TSA	0.000125814	0.00030199	0.000113
	SSA	0.002714397	0.00018865	0.000210
	MVO	0.000191389	0.00019053	0.000477

Candidate Optimizer (SCO). The objective of this strategy is to accurately estimate the unknown parameters in various PV models. The methodology being offered utilizes the robust exploratory capacity of the CSCO technique in conjunction with the operational local search capability of the SCO process. The efficacy of the suggested methodology is assessed through the utilization of a diverse range of unimodal and multimodal benchmark functions. The findings indicate that, in most test functions, the CSCSC technique exhibits greater performance in accomplishing global explanatory objectives compared to the basic SCO approach and other approaches. The mean RMSE values generated by CSCSC are 9.86E−04, 9.8625E−04, and 4.443E−03 for SDM, DDM, and PVM, respectively. The proposed CSCSC approach is subsequently utilized to acquire the PV model parameters that result in the lowest RMSE. Based on the empirical findings, it can be inferred that the solutions produced by the proposed CSCSC demonstrate a superior degree of efficacy in the optimization and operation of practical solar systems in comparison to the algorithms employed for comparative analysis. The results obtained from the contrasting simulation indicate that CSCSC demonstrates competence in performing accurate and reliable parameter estimation. The suggested CSCSC algorithm can also be used in a variety of domains, including decision-making, wireless networks, structural optimization, power and energy systems, energy forecasting, and re-selection. This research's future focus is also thought to be on the binary and hybrid forms of CSCSC. Additionally, it is suggested that in a future study, economics be considered an objective function.

Conflict of Interest

There is no conflict of interest.

Supporting Information

Not applicable.

References

[1] B. Yang, T. Yu, H. Shu, Y. Zhang, J. Chen, Y. Sang, L. Jiang, Passivity-based sliding-mode control design for optimal power extraction of a PMSG based variable speed wind turbine, *Renewable Energy*, 2018, **119**, 577-589, doi: 10.1016/j.renene.2017.12.047.

[2] M. R. Gomaa, A. K. Al-Bawwat, M. Al-Dhaifallah, H. Rezk, M. Ahmed, Optimal design and economic analysis of a hybrid renewable energy system for powering and desalinating seawater, *Energy Reports*, 2023, **9**, 2473-2493, doi:

10.1016/j.egyr.2023.01.087.
[3] E. T. Sayed, H. Rezk, A. G. Olabi, M. R. Gomaa, Y. B. Hassan, S. M. Atiqure Rahman, S. K. Shah, M. Ali Abdelkareem, Application of artificial intelligence to improve the thermal energy and exergy of nanofluid-based pv thermal/nano-enhanced phase change material, *Energies*, 2022, **15**, 8494, doi: 10.3390/en15228494.
[4] H. Al-Rawashdeh, O. Ali Al-Khashman, L. M. Arrfou, M. R. Gomaa, H Rezk, M. Shalby, J. T. Al Bdour, M. Louzazni, Different scenarios for reducing carbon emissions optimal sizing, and design of a stand-alone hybrid renewable energy system for irrigation purposes, *International Journal of Energy Research*, 2023, **2023**, 6338448, doi; 10.1155/2023/6338448.
[5] H. Al-Rawashdeh,O. Ali Al-Khashman, J. T. Al Bdour, M. R. Gomaa, H. Rezk, A. Marashli, L. M. Arrfou, M. Louzazni, Performance analysis of a hybrid renewable-energy system for green buildings to improve efficiency and reduce GHG emissions with multiple scenarios, *Sustainability*, 2023, **15**, 7529, doi: 10.3390/su15097529.
[6] D. Oliva, E. Cuevas, G. Pajares, Parameter identification of solar cells using artificial bee colony optimization, *Energy*, 2014, **72**, 93-102, doi: 10.1016/j.energy.2014.05.011.
[7] A. Noori, M. J. Shahbazadeh, M. Eslami, Designing of wide-area damping controller for stability improvement in a large-scale power system in presence of wind farms and SMES compensator, *International Journal of Electrical Power & Energy Systems*, 2020, **119**, 105936, doi: 10.1016/j.ijepes.2020.105936.
[8] J, Siecker, A review of solar photovoltaic systems cooling technologies, *Renewable and Sustainable Energy Reviews*, 2017, **79**, 192-203, doi: 10.1016/j.rser.2017.05.053.
[9] Xi, Yang, Comparative study on parameter extraction of photovoltaic models via differential evolution, *Energy Conversion and Management*, 2019, **201**, 112113, doi: 10.1016/j.enconman.2019.112113.
[10] H. Mohammed, Qais, Enhanced whale optimization algorithm for maximum power point tracking of variable-speed wind generators, *Applied Soft Computing*, 2020, **86**, 105937, doi: 10.1016/j.asoc.2019.105937.
[11] H. M. Ridha, Parameters extraction of single and double diodes photovoltaic models using Marine Predators Algorithm and Lambert W function, *Solar Energy*, 2020, **209**, 674-693, doi: 10.1016/j.solener.2020.09.047.
[12] V. Jack, Chin, Cell modelling and model parameters estimation techniques for photovoltaic simulator application: a review, *Applied Energy*, 2015, **154**, 500-519, doi: 10.1016/j.apenergy.2015.05.035.
[13] H. Chen, S. Jiao, M. Wang, A. A. Heidari, X. Zhao, Parameters identification of photovoltaic cells and modules using diversification-enriched Harris Hawks optimization with chaotic drifts, *Journal of Cleaner Production*, 2020, **244**, 118778, doi: 10.1016/j.jclepro.2019.118778.
[14] M. Merchaoui, A. Sakly, M. F. Mimouni, Particle swarm optimisation with adaptive mutation strategy for photovoltaic solar cell/module parameter extraction, *Energy Conversion and Management*, 2018, **175**, 151-163, doi: 10.1016/j.enconman.2018.08.081.
[15] Youssef, Kharchouf, Parameter's extraction of solar photovoltaic models using an improved differential evolution algorithm, *Energy Conversion and Management*, 2022, **251**, 114972, doi: 10.1016/j.enconman.2021.114972.
[16] T. Easwarakhanthan, J. Bottin, I. Bouhouch, C. Boutrit, Nonlinear minimization algorithm for determining the solar cell parameters with microcomputers, *International Journal of Solar Energy*, 1986, **4**, 1-12, doi: 10.1080/01425918608909835.
[17] J. Liang, S. Ge, B. Qu, K. Yu, F. Liu, H. Yang, P. Wei, Z. Li, Classified perturbation mutation based particle swarm optimization algorithm for parameters extraction of photovoltaic models, *Energy Conversion and Management*, 2020, **203**, 112138, doi: 10.1016/j.enconman.2019.112138.
[18] K. M. El-Naggar, M. R. AlRashidi, M. F. AlHajri, A. K. Al-Othman, Simulated Annealing algorithm for photovoltaic parameters identification, *Solar Energy*, 2012, **86**, 266-274, doi: 10.1016/j.solener.2011.09.032.
[19] A. Askarzadeh, A. Rezazadeh, Parameter identification for solar cell models using harmony search-based algorithms, *Solar Energy*, 2012, **86**, 3241-3249, doi: 10.1016/j.solener.2012.08.018.
[20] N. Rajasekar, N. Krishna Kumar, R. Venugopalan, Bacterial Foraging Algorithm based solar PV parameter estimation, *Solar Energy*, 2013, **97**, 255-265, doi: 10.1016/j.solener.2013.08.019.
[21] Wen, Long, A new hybrid algorithm based on grey wolf optimizer and cuckoo search for parameter extraction of solar photovoltaic models, *Energy Conversion and Management*, 2020, **203**, 112243, doi: 10.1016/j.enconman.2019.112243.
[22] Lei, Guo, Parameter identification and sensitivity analysis of solar cell models with cat swarm optimization algorithm, *Energy Conversion and Management*, 2016, **108**, 520-528, doi: 10.1016/j.enconman.2015.11.041.
[23] Shuijia, Li, An enhanced adaptive differential evolution algorithm for parameter extraction of photovoltaic models, *Energy Conversion and Management*, 2020, **205**, 112443, doi: 10.1016/j.enconman.2019.112443.
[24] Guojiang, Xiong, Parameter extraction of solar photovoltaic models using an improved whale optimization algorithm, *Energy Conversion and Management*, 2018, **174**, 388-405, doi: 10.1016/j.enconman.2018.08.053.
[25] A. Mohammad, Beigi, Parameter identification for solar cells and module using a Hybrid Firefly and Pattern Search Algorithms, *Solar Energy*, 2018, **171**, 435-446, doi: 10.1016/j.solener.2018.06.092.
[26] D. Allam, D. Yousri, M. Eteiba, Parameters extraction of the three diode model for the multi-crystalline solar cell/module using Moth-Flame Optimization Algorithm, *Energy Conversion and Management*, 2016, **123**, 535-548, doi: 10.1016/j.enconman.2016.06.052.
[27] Satnam, Kaur, Tunicate Swarm Algorithm: a new bio-inspired based metaheuristic paradigm for global optimization, *Engineering Applications of Artificial Intelligence*, 2020, **90**, 103541, doi: 10.1016/j.engappai.2020.103541.

[28] S. Mirjalili, S. M. Mirjalili, A. Hatamlou, Multi-Verse Optimizer: a nature-inspired algorithm for global optimization, *Neural Computing and Applications*, 2016, **27**, 495-513, doi: 10.1007/s00521-015-1870-7.
[29] M. Noroozi, H. Mohammadi, E. Efatinasab, A. Lashgari, M. Eslami, B. Khan, Golden search optimization algorithm, *IEEE Access*, 2022, **10**, 37515-37532, doi: 10.1109/access.2022.3162853.
[30] M. Premkumar, N. Shankar, R. Sowmya, P. Jangir, C. Kumar, L. Abualigah, B. Derebew, A reliable optimization framework for parameter identification of single-diode solar photovoltaic model using weighted velocity-guided grey wolf optimization algorithm and Lambert-W function, *IET Renewable Power Generation*, 2023, **17**, 2711-2732, doi: 10.1049/rpg2.12792.
[31] M. Premkumar, P. Jangir, R. Sowmya, Parameter extraction of three-diode solar photovoltaic model using a new metaheuristic resistance-capacitance optimization algorithm and improved Newton-Raphson method, *Journal of Computational Electronics*, 2023, **22**, 439-470, doi: 10.1007/s10825-022-01987-6.
[32] M, Premkumar, An enhanced Gradient-based Optimizer for parameter estimation of various solar photovoltaic models, *Energy Reports*, 2022, **8**, 15249-15285, doi: 10.1016/j.egyr.2022.11.092.
[33] P. Manoharan, S. Ravichandran, P. Jangir, ZRMSE: a new and reliable approach for computing the circuit parameters of single-diode solar photovoltaic model, 2022 IEEE 2nd International Conference on Sustainable Energy and Future Electric Transportation (SeFeT), IEEE, 2022, 1-7.
[34] M. Premkumar, P. Jangir, R. Sowmya, R. M. Elavarasan, B. S. Kumar, Enhanced chaotic JAYA algorithm for parameter estimation of photovoltaic cell/modules, *ISA Transactions*, 2021, **116**, 139-166, doi: 10.1016/j.isatra.2021.01.045.
[35] M. Yaghoubi, M. Eslami, M. Noroozi, H. Mohammadi, O. Kamari, S. Palani, Modified salp swarm optimization for parameter estimation of solar PV models, *IEEE Access*, 2022, **10**, 110181-110194, doi: 10.1109/ACCESS.2022.3213746.
[36] M. Eslami, E. Akbari, S. T. Seyed Sadr, B. F. Ibrahim, A novel hybrid algorithm based on rat swarm optimization and pattern search for parameter extraction of solar photovoltaic models, *Energy Science & Engineering*, 2022, **10**, 2689-2713, doi: 10.1002/ese3.1160.
[37] B. Arandian, M. Eslami, S. A. Khalid, B. Khan, U. U. Sheikh, E. Akbari, A. H. Mohammed, An effective optimization algorithm for parameters identification of photovoltaic models, *IEEE Access*, 2022, **10**, 34069-34084, doi: 10.1109/ACCESS.2022.3161467.
[38] S. M, Ismail, Characterization of PV panel and global optimization of its model parameters using genetic algorithm, *Energy Conversion and Management*, 2013, **73**, 10-25, doi: 10.1016/j.enconman.2013.03.033.
[39] J. Kennedy, R. Eberhart, Particle swarm optimization. Proceedings of ICNN'95 - International Conference on Neural Networks. November 27 - December 1, 1995, Perth, WA, Australia. IEEE, 2002, 1942-1948, doi: 10.1109/ICNN.1995.488968.
[40] Kunjie, Yu, Parameters identification of photovoltaic models using an improved JAYA optimization algorithm, *Energy Conversion and Management*, 2017, **150**, 742-753, doi: 10.1016/j.enconman.2017.08.063.
[41] A. Sharma, A. Dasgotra, S. K. Tiwari, A. Sharma, V. Jately, B. Azzopardi, Parameter extraction of photovoltaic module using tunicate swarm algorithm, *Electronics*, 2021, **10**, 878, doi: 10.3390/electronics10080878.
[42] M. Premkumar, P. Jangir, C. Kumar, S. David Thanasingh Sundarsingh Jebaseelan, H. H. Alhelou, R. Madurai Elavarasan, H. Chen, Constraint estimation in three-diode solar photovoltaic model using Gaussian and Cauchy mutation-based hunger games search optimizer and enhanced Newton-Raphson method, *IET Renewable Power Generation*, 2022, **16**, 1733-1772, doi: 10.1049/rpg2.12475.
[43] Seyedali, Mirjalili, Salp Swarm Algorithm: a bio-inspired optimizer for engineering design problems, *Advances in Engineering Software*, 2017, **114**, 163-191, doi: 10.1016/j.advengsoft.2017.07.002.
[44] M. Khajehzadeh, M. R. Taha, M. Eslami, A new hybrid firefly algorithm for foundation optimization, *National Academy Science Letters*, 2013, **36**, 279-288, doi: 10.1007/s40009-013-0129-z.
[45] M. Khajehzadeh, M. R. Taha, M. Eslami, Efficient gravitational search algorithm for optimum design of retaining walls, *Structural Engineering and Mechanics*, 2013, **45**, 111-127, doi: 10.12989/sem.2013.45.1.111.
[46] M. Khajehzadeh, M. Taha, A. El-Shafie, M. Eslami, Search for critical failure surface in slope stability analysis by gravitational search algorithm, *International Journal of Physical Sciences*, 2011, **6**, 5012-5021.
[47] M. Khajehzadeh, M. R. Taha, M. Eslami, Multi-objective optimisation of retaining walls using hybrid adaptive gravitational search algorithm, *Civil Engineering and Environmental Systems*, 2014, **31**, 229-242, doi: 10.1080/10286608.2013.853746.
[48] A. Seyyedabbasi, F. Kiani, Sand Cat swarm optimization: a nature-inspired algorithm to solve global optimization problems, *Engineering With Computers*, 2023, **39**, 2627-2651, doi: 10.1007/s00366-022-01604-x.
[49] E. D. Dolan, R. M. Lewis, V. Torczon, On the local convergence of pattern search, *SIAM Journal on Optimization*, 2003, **14**, 567-583, doi: 10.1137/s1052623400374495.
[50] G. Huang, J. Rosowski, M. Ravicz, W. Peake, Mammalian ear specializations in arid habitats: structural and functional evidence from sand cat (Felis margarita), *Journal of Comparative Physiology A*, 2002, **188**, 663-681, doi: 10.1007/s00359-002-0332-8.
[51] I. Cherki, A. Chaker, Z. Djidar, N. Khalfallah, F. Benzergua, A sequential hybridization of genetic algorithm and particle swarm optimization for the optimal reactive power flow, *Sustainability*, 2019, **11**, 3862, doi: 10.3390/su11143862.

[52] M. R. AlRashidi, M. F. AlHajri, K. M. El-Naggar, A. K. Al-Othman, A new estimation approach for determining the I-V characteristics of solar cells, *Solar Energy*, 2011, **85**, 1543-1550, doi: 10.1016/j.solener.2011.04.013.
[53] A. Rezaee, Jordehi, Parameter estimation of solar photovoltaic (PV) cells: a review, *Renewable and Sustainable Energy Reviews*, 2016, **61**, 354-371, doi: 10.1016/j.rser.2016.03.049.
[54] H. G. G. Nunes, J. A. N. Pombo, P. M. R. Bento, S. J. P. S. Mariano, M. R. A. Calado, Collaborative swarm intelligence to estimate PV parameters, *Energy Conversion and Management*, 2019, **185**, 866-890, doi: 10.1016/j.enconman.2019.02.003.
[55] H. Tian, F. Mancilla-David, K. Ellis, E. Muljadi, P. Jenkins, A cell-to-module-to-array detailed model for photovoltaic panels, *Solar Energy*, 2012, **86**, 2695-2706, doi: 10.1016/j.solener.2012.06.004.
[56] K. Zervoudakis, S. Tsafarakis, A mayfly optimization algorithm, *Computers & Industrial Engineering*, 2020, **145**, 106559, doi: 10.1016/j.cie.2020.106559.
[57] Qun, Niu, An improved TLBO with elite strategy for parameters identification of PEM fuel cell and solar cell models, *International Journal of Hydrogen Energy*, 2014, **39**, 3837-3854, doi: 10.1016/j.ijhydene.2013.12.110.
[58] X. Chen, K. Yu, W. Du, W. Zhao, G. Liu, Parameters identification of solar cell models using generalized oppositional teaching learning-based optimization, *Energy*, 2016, **99**, 170-180, doi: 10.1016/j.energy.2016.01.052.
[59] Z. Wu, D. Yu, X. Kang, Parameter identification of photovoltaic cell model based on improved ant lion optimizer, *Energy Conversion and Management*, 2017, **151**, 107-115, doi: 10.1016/j.enconman.2017.08.088.
[60] S. J. Patel, A. Panchal, V. Kheraj, Extraction of solar cell parameters from a single current–voltage characteristic using teaching learning-based optimization algorithm, *Applied Energy*, 2014, **119**, 384-393, doi: 10.1016/J.APENERGY.2014.01.027.

